



**University of
Zurich^{UZH}**

**Zurich Open Repository and
Archive**

University of Zurich
University Library
Strickhofstrasse 39
CH-8057 Zurich
www.zora.uzh.ch

Year: 2011

Modeling of pathological traits in Alzheimer's disease based on systemic extracellular signaling proteome

Britschgi, M ; Rufibach, K ; Bauer Huang, S L ; Clark, C M ; Kaye, J A ; Li, G ; Peskind, E R ; Quinn, J F ; Galasko, D R ; Wyss-Coray, T

Abstract: The study of chronic brain diseases including Alzheimer's disease in patients is typically limited to brain imaging or psychometric testing. Given the epidemic rise and insufficient knowledge about pathological pathways in sporadic Alzheimer's disease, new tools are required to identify the molecular changes underlying this disease. We hypothesize that levels of specific secreted cellular signaling proteins in cerebrospinal fluid or plasma correlate with pathological changes in the Alzheimer's disease brain and can thus be used to discover signaling pathways altered in the disease. Here we measured 91 proteins of this subset of the cellular communication proteome in plasma or cerebrospinal fluid in patients with Alzheimer's disease and cognitively normal controls to mathematically model disease-specific molecular traits. We found small numbers of signaling proteins that were able to model key pathological markers of Alzheimer's disease, including levels of cerebrospinal fluid -amyloid and tau, and classify disease in independent samples. Several of these factors had previously been implicated in Alzheimer's disease supporting the validity of our approach. Our study also points to proteins which were previously unknown to be associated with Alzheimer's disease thereby implicating novel signaling pathways in this disorder.

DOI: <https://doi.org/10.1074/mcp.M111.008862>

Posted at the Zurich Open Repository and Archive, University of Zurich

ZORA URL: <https://doi.org/10.5167/uzh-51047>

Journal Article

Accepted Version

Originally published at:

Britschgi, M; Rufibach, K; Bauer Huang, S L; Clark, C M; Kaye, J A; Li, G; Peskind, E R; Quinn, J F; Galasko, D R; Wyss-Coray, T (2011). Modeling of pathological traits in Alzheimer's disease based on systemic extracellular signaling proteome. *Molecular Cellular Proteomics*, 10(10):1-11.

DOI: <https://doi.org/10.1074/mcp.M111.008862>

Modeling of pathological traits in Alzheimer's disease based on systemic extracellular signaling proteome

Markus Britschgi^{1#*}, Kaspar Rufibach², Sarah L. Bauer Huang¹, Christopher M. Clark³, Jeffrey A. Kaye⁴, Ge Li⁵, Elaine R. Peskind^{5,6}, Joseph F. Quinn⁴, Douglas R. Galasko⁷, and Tony Wyss-Coray^{1,8*}

¹ Department of Neurology and Neurological Sciences, Stanford University School of Medicine, 300 Pasteur Drive, Rm A343, Stanford, CA 94305-5235, USA

² Institute of Social- and Preventive Medicine, Division of Biostatistics, University of Zurich, Hirschengraben 84, CH-8001 Zurich, Switzerland

³ Department of Neurology, Alzheimer's Disease Center, and Institute on Aging, University of Pennsylvania, 3615 Chestnut Street Philadelphia, PA 19104, USA

⁴ Layton Aging & Alzheimer's Disease Center, Oregon Health Sciences University, 3181p SW Sam Jackson Park Road, CR131, Portland, OR 97201-3098, USA

⁵ Dept. of Psychiatry and Behavioral Sciences, University of Washington, School of Medicine, Seattle, WA 98108-1597, USA

⁶ Veterans Affairs Northwest Network Mental Illness Research, Education, and Clinical Center, Seattle, WA 98108-1597, USA

⁷ Department of Neurosciences, University of California San Diego, 9500 Gilman Drive # 9127, La Jolla, CA 92093-9127, USA

⁸ Center for Tissue Regeneration, Repair and Restoration, Veterans Affairs Palo Alto Health Care System, 3801 Miranda Ave, Palo Alto, CA 94304, USA

Current address: CNS Discovery, pRED, F. Hoffmann-La Roche Ltd., Basel, Switzerland

Corresponding authors

* Tony Wyss-Coray, Stanford University School of Medicine, Department of Neurology and Neurological Sciences, 300 Pasteur Drive, Rm A343, Stanford, CA 94305-5235, USA, phone: (650) 852-3220, fax: (650) 849 0434, e-mail: twc@stanford.edu

* Markus Britschgi, F. Hoffmann-La Roche Ltd, pRED, CNS Discovery, Grenzacherstrasse 124, 4070 Basel, Switzerland, phone: +41 61 687 9116, fax: +41 61 688 90 60, e-mail: markus.britschgi@roche.com

RUNNING TITLE: Abnormal systemic protein networks in Alzheimer's disease

ABBREVIATIONS

A β , β -amyloid

AD, Alzheimer's disease

AUC, area under the curve

BBB, blood-brain barrier

CSF, cerebrospinal fluid

E-net, Elastic net

MCI, mild cognitive impairment

NDC, non-demented controls

p-tau₁₈₁, tau phosphorylated at threonine 181

RC, regression coefficient

R_s , Spearman Rank correlation coefficient

t-tau, total tau

CLSI, Clinical Laboratory Standards Institute

Abbreviations of all measured proteins are listed separately in Supplemental Table S2.

SUMMARY

The study of chronic brain diseases including Alzheimer's disease in patients is typically limited to brain imaging or psychometric testing. Given the epidemic rise and insufficient knowledge about pathological pathways in sporadic Alzheimer's disease, new tools are required to identify the molecular changes underlying this disease. We hypothesize that levels of specific secreted cellular signaling proteins in cerebrospinal fluid or plasma correlate with pathological changes in the AD brain and can thus be used to discover signaling pathways altered in the disease. Here we measured 91 proteins of this subset of this cellular communication proteome in plasma or cerebrospinal fluid in patients with Alzheimer's disease and cognitively normal controls to mathematically model disease-specific molecular traits. We found small numbers of signaling proteins that were able to model key pathological markers of Alzheimer's disease, including levels of cerebrospinal fluid β -amyloid and tau, and classify disease in independent samples. Several of these factors had previously been implicated in Alzheimer's disease supporting the validity of our approach. Our study also points to proteins which were previously unknown to be associated with Alzheimer's disease thereby implicating *novel* signaling pathways in this disorder.

INTRODUCTION

The brain regulates key biological processes throughout the organism by releasing molecules into the blood and cerebrospinal fluid (CSF), and systemic factors in turn can induce cognitive and behavioral changes in animals and humans (1, 2). Thus, brain and periphery are interconnected not only on a cellular level but also in a complex molecular network of soluble communication factors.

Alzheimer's disease (AD) is the most common form of dementia affecting an estimated 5.4 million individuals in the US (3). The cause of AD is not known but genetic and pathological studies point to a key role for cerebral β -amyloid ($A\beta$) peptide and hyperphosphorylated tau in the disease. Levels of soluble $A\beta_{42}$ in CSF decrease in AD in parallel to its deposition into amyloid plaques in the brain parenchyma, whereas tau increases as the disease progresses making these proteins good biomarkers of AD (4-6). Moreover, ratios between the concentrations of tau phosphorylated at threonine 181 ($p\text{-tau}_{181}$) and total tau ($t\text{-tau}$) or $A\beta_{42}$ are predictive of future development of AD in patients with mild cognitive impairment (MCI) (7-9) and cognitive decline (10-12) or brain atrophy in non-demented older adults (13). Despite the usefulness of these CSF markers in the diagnosis of AD patients (4, 5), they provide little information on biological mechanisms involved in this disorder.

Some members of the molecular network which include cytokines, chemokines, or growth factors have been reported to have different expression levels in patients with neurological diseases compared to those found in healthy controls [reviewed in (14)]. We and others have measured in plasma or CSF from AD patients and controls large numbers of communication factors, which we collectively called the *communicome*, and by statistically comparing levels in AD patients versus levels in controls we identified small groups of factors that could form a signature for the disease (15-19). Together, these findings point to e.g. abnormal transcriptional regulation of peripheral leukocytes (20, 21) or neuroinflammatory pathways in AD (22). Technical problems and small sample sizes, however, have made it difficult to identify proteins, which are predictive of AD across various centers and studies (18) and the two-class analysis approach (AD patients versus a control group) is appealing for finding differences but provides little insight into the role of these markers in AD.

Here we propose an alternative analytical approach in which levels of communication factors in CSF and plasma are used to mathematically model levels of $A\beta_{42}$ and tau. We do this based on the hypothesis that the systemic network of the extracellular signaling proteome is linked with the levels of CSF markers of AD pathology and indicators of disease progression. The findings could help in identifying proteins and biological pathways hitherto unknown to be involved in AD.

EXPERIMENTAL PROCEDURES

Subjects and APOE genotyping. AD patients and healthy non-demented controls (NDC) (**Table S1**) were recruited for multicentre studies that aim to identify molecular biomarkers for AD in blood and CSF. Subjects were chosen based on standardized inclusion and exclusion criteria (see **Supplemental Methods**). Written informed consent was obtained from all subjects, or assent from subjects and consent from caregivers in the case of subjects with significant impaired decisional capacity, in accordance with institutional ethics committee review boards at each participating institution. *APOE* genotyping was performed by the restriction digest method (23).

Collection of CSF and plasma. CSF and plasma samples were generated by standard procedures as described (19, 24). Briefly, for the majority of patients lumbar puncture and blood draw was conducted between 9am and 11am after an overnight fast. After blood draw into K2-EDTA-coated lavender top vacutainers, blood was kept on ice, spun at 1000g in a refrigerated centrifuge within one hour of draw, aliquoted, and frozen on dry ice. All samples were stored at -80°C until use with no previous thaw cycle.

Measurement of analytes in CSF and plasma. We measured CSF levels of A β 42, t-tau, and p-tau₁₈₁ by Luminex xMAP method (AlzBio3, Innogenetics, Ghent, Belgium) a bead-based sandwich immunoassay. Plasma samples were shipped from Seattle to Palo Alto where they were thawed and aliquoted. For the multi-analyte profiling plasma aliquots were sent to Rules-Based Medicine (RBM, Austin, Texas) and measured in two big batches of samples from NDC and AD patients. CSF was sent directly to RBM and analyzed in one experiment. All samples were analyzed blinded by robotic sample handlers in a bead-based multiplex sandwich immunoassay (Luminex bead analyzer), according to Clinical Laboratory Standards Institute (CLSI) guidelines and rigorous assessment of fundamental assay parameters (<http://www.rulesbasedmedicine.com/quality-policy/data-quality/>). Out of 90 analytes measured by RBM IFN- γ , IGF-1, IL-1 α , and lipoprotein-a were not detectable in any of the CSF and plasma samples. Additional analytes were excluded if they were detectable in less than 10% of samples. This resulted in 73 detectable proteins in each, plasma and CSF, with 60 proteins overlapping between the two biological fluids (**Table S2**). Soares and colleagues reported a similar sensitivity of this platform (18). As a quality control we remeasured 35 plasma samples at RBM 17 months after the initial plasma measurements. 86% of the detectable analytes correlated between the two measurements with a Pearson correlation coefficient $R \geq 0.7$ (52% $R \geq 0.9$, 34% $R = 0.7-0.9$) and 14% with $R < 0.7$. Lower R-values were due to changes in assay settings in the second experiment, which rendered most values for these

analytes below least detectable dose or undetectable. Nevertheless, these data generated at two independent time points made us confident, that RBM produces highly reproducible data. Also, analytes with low correlation coefficient were deemed suitable for analysis because in the first experiment they were well above detection limit. Only data from the first experiment were subsequently used for the analysis. In addition, plasma levels of MCSF were quantified separately by Quantikine ELISA (R&D Systems, Minneapolis, USA) and were detectable in all plasma samples.

Statistical analysis. Analysis was done in Prism 5 and R [<http://www.r-project.org/>, (25)]. The entire plasma sample set contained 78 AD patients and 118 NDC (**Table S1**) and we measured levels of tau, p-tau₁₈₁, and A β 42 in 72 AD patients and 112 controls. We standardized the values to z-scores by subtracting the mean and dividing by the standard deviation (26). Measurements below lowest detectable protein concentration were imputed conservatively with the lowest available value of an analyte. Values missing at random (e.g. analyte not measured due to insufficient amounts of sample) were imputed with 0 (which is the mean of the available observations) after standardization. The entire plasma set was randomly split into a training set (79 NDC, 52 AD) and a test set (39 NDC, 26 AD), whereby we insisted on the same AD versus NDC frequency distribution in the training and test as in the entire dataset and that all subjects in the training set have measurements for A β 42 and tau. The CSF sample set was analyzed without further splitting. For the CSF sample set and the plasma training set high-dimensional linear regression models for continuous endpoints were computed with an *elastic net penalty* [<http://cran.r-project.org/web/packages/elasticnet/index.html>, (27)] using the add-on package *elasticnet*. We used the standardized levels of t-tau, p-tau₁₈₁, A β 42, or the ratios of A β 42/t-tau, or A β 42/p-tau₁₈₁, respectively, as the continuous response variables in the linear regression equation and the standardized values of CSF or plasma protein levels together with sex and risk factors for AD APOE genotype and age as the explanatory variables. The penalty parameter was chosen via 10-fold cross validation minimizing prediction error. For fixed alpha, the regularization parameter lambda is varied from lambda_{max}, the smallest lambda such that all coefficients are estimated without constraint, down to a very small lambda_{min}; lambda = 0 renders the algorithm unstable (28). We use the built-in specification of lambdas that automatically chooses a suitable number of lambdas in the interval [lambda_{min}, lambda_{max}]. For alpha we used {0.01, 0.2, 0.4, 0.6, 0.8, 1}. Alpha = 1 specifies a pure Lasso penalty. For each response a separate model was calculated (**Table I**, Model C1-5 in CSF, P6-8 in plasma) and variables that fitted best into the corresponding model (selected predictors) are listed in order of decreasing association to the response variable

(absolute size of regression coefficient, RC). To test the diagnostic utility of the selected predictors in both the training and the test set, we used the selected predictors to model the binary endpoint AD versus NDC (based on clinical diagnosis) and calculated a ROC curve where the linear predictor from the logistic regression was the continuous variable. This was compared to the ROC curve that is based on models with t-tau, p-tau_{181p}, A β 42, and their ratios A β 42/t-tau, and A β 42/p-tau_{181p}, respectively. Comparison of the logistic regression analyses was done via ROC with 95% Wald-type confidence intervals for AUC on logit-scale were computed using the approach of Hanley and McNeil (29, 30). To assess the risk associated with *APOE* genotype we computed an ordinary logistic regression model with dependent variable AD versus non-AD and explanatory variable *APOE4* status (ϵ 4 versus non- ϵ 4). In addition to the odds ratio we report a 95% profile likelihood confidence interval.

Connectivity network diagrams. First, we calculated the Spearman rank correlation coefficients (R_s) between all analytes in separate correlation matrices for AD patients and NDC, respectively. Confidence intervals for R_s between analytes in plasma and CSF were calculated using Fisher's z-transformation and t-quantiles. The R_s is an indicator of connectivity of two analytes and R_s ranges [0.4,1] and [-1,-0.4] were used to draw connectivity network diagrams for selected analytes. To quantify the strength of integration of an analyte in the connectivity network we calculated for each analyte an interaction score, which is the sum of the squared values of all R_s in the range of [-1,1] between this analyte and all analytes in the connectivity diagram.

RESULTS

Two thirds of measured communication factors are detectable in CSF.

We measured the concentrations of 91 secreted proteins in plasma from 78 AD patients and 118 cognitively normal elderly NDCs; we also measured 90 proteins in CSF of 25 AD patients and 18 NDC (**Table S1** and **S2**). These proteins represent some of the best-studied cytokines, chemokines, growth factors, and acute phase response proteins and were selected based on availability in multiplex sandwich immunoassay. Seventy-four proteins were detectable in plasma and 73 in CSF, with 60 proteins overlapping between the two biological fluids. Protein concentrations were generally lower in CSF than in plasma (between 5- to 8000-fold) with a few interesting exceptions. β 2-microglobulin, CD40, CCL11/eotaxin, tissue inhibitor of metalloproteinase (TIMP)-1, or tissue factor (TF) were measured at similar concentrations in both fluids and levels of fatty acid binding protein 3 (FABP3), CCL2/monocyte chemotactic protein-1

(MCP-1), CXCL8/interleukin-8, and vascular endothelial growth factor (VEGF) were 1.5- to 10-times higher in CSF than in plasma. These observations indicate that a majority of the communication factors, many known classically for their role in peripheral immune function, developmental processes, or systemic diseases, may have a function in the CNS as well.

CSF communication factors can model CSF A β and tau and hence discriminate between AD and NDC.

Consistent with published reports (9, 11, 31) CSF levels of A β 42, t-tau, p-tau₁₈₁ alone or in combination were strong classifiers of AD in our data set (area under the curve (AUC) 0.75-0.90 for various models; **Table II**). If levels of communication factors are indeed associated with the disease process (discussed in (6)) they should be able to model the pathological changes characteristic of AD (**Fig 1**). We thus modeled levels of CSF A β 42, t-tau, p-tau₁₈₁, or ratios A β 42/t-tau or A β 42/p-tau₁₈₁ with all measurements of communication factors in CSF (73 detectable factors) using the linear regression-modeling tool *Elastic net* (E-net, (27)). We adjusted for sex and AD risk factors age and *APOE4* status by including them as variables in the analysis. In E-net models C1–C5 a total of 12 CSF proteins were selected to be associated with the 5 pathological markers of AD. Interestingly, FABP3 and creatine kinase-muscle/brain (CK-MB), showed a consistently strong association in all models involving tau; (indicated by shades of green in **Table I**) endothelin-1, and interleukin-13 (IL-13) were also required to model p-tau₁₈₁. IL-7 was the only factor selected to model A β 42 but with a regression coefficient of nearly zero, implying that its influence on the response variable in the regression model is small.

The communication factors selected in E-net Models C2 and C5 (the latter in conjunction with *APOE4* status) were capable of independently classifying AD and NDC similar to or slightly better than p-tau₁₈₁ or A β 42/p-tau₁₈₁ levels measured in these patients (**Fig 2A,B** and **Table II**). This validates the chosen communication proteins and suggests that they are biologically related to the abundance of p-tau₁₈₁ and A β 42 in CSF, the pathological hallmarks of AD.

Consistent with the E-net analysis, we observed in the connectivity network diagram of the overall 12 selected CSF communication factors strong, positive Spearman rank correlations (R_s) between t-tau or p-tau₁₈₁ and a number of communication factors in healthy individuals but A β 42 was only weakly integrated into this network (**Fig 2C**). Other factors including CXCL8, FABP3, matrix metalloproteinase 3 (MMP-3), and stem cell factor (SCF) show strong correlations with each other in this network ($R_s \geq 0.8$). While some of these relationships are maintained in AD (FABP3, MMP-3, SCF), the strong correlations with tau are missing; instead, negative relationships between tau, CK-MB, and TNF- β appear, and C-reactive protein (CRP) becomes a network hub with

several positive interactions (**Fig 2D**). This change in connectivity between pathological and communication factors in AD versus NDC is reflected by differences in the interaction scores.

Plasma communication factors can model CSF tau and A β and hence discriminate between AD and NDC.

We next asked whether blood-derived proteins have a relationship to CSF pathological markers of AD and may thus be related to the disease itself (**Fig 1**). We again used E-net to model A β ₄₂, t-tau, p-tau₁₈₁, or ratios A β ₄₂/t-tau or A β ₄₂/p-tau₁₈₁ but this time based on values for 74 detectable plasma communication proteins (**Table S2**) in a training set of 52 AD patients and 79 NDC (**Table S1**), and we adjusted for sex, age and *APOE4* status. A total of 22 plasma communication factors were selected to best model pathological CSF markers in E-net Models P6–P10 (**Table I**). Notably, CK-MB and tumor necrosis factor- β (TNF- β) overlapped with proteins selected in the CSF models. Among the 22 proteins, macrophage-colony stimulating factor (MCSF) showed the strongest and most consistent association with all 5 pathological markers in CSF although *APOE4* status and age were key drivers in two of these models (P8, P9). Other prominent factors were selected in four models (CK-MB and granulocyte-colony stimulating factor (G-CSF)) or in three models (TNF-RII, IL-3 and PAI-1) (indicated by shades of orange in **Table I**).

To assess the potential diagnostic utility of the selected plasma proteins we calculated ROC curves for the training set. Several models outperformed the pathological CSF markers in classifying NDC and AD, and this effect was not simply explained by *APOE4* status and age (**Table II** and **Fig 3A,C**). Moreover, plasma communication factors in combination with *APOE4* status and age were as effective in classifying AD as CSF measurements of A β ₄₂/tau and A β ₄₂/p-tau₁₈₁ (**Table II**). We validated the results of these models in an independent test set with 65 subjects (**Table S1**), producing a classification (AUC 0.74-0.77), which was clearly stronger than with *APOE4* status and age alone (AUC 0.63, **Fig 3B,D**).

Consistent with the E-net analysis, connectivity network diagrams illustrated a considerable complexity of relationships between all 22 plasma communication factors selected by E-net models P6–P10 and tau and A β in NDC (**Fig 4A**). Interestingly, this network becomes seemingly more complex in AD subjects where immune and inflammatory factors become important network hubs (**Fig 4B**). For example, β 2-microglobulin shows strong correlations with inflammatory factors TIMP-1, PAI-1 and members of the TNF superfamily (CD40L, TNF RII, and TNF- β) in the AD network.

Correlations and connectivity between communication factors in CSF and plasma are altered in AD.

To assess whether levels of a given protein factor in the CSF are related to its levels in plasma we compared CSF and plasma concentrations in 43 subjects using Spearman rank correlation. In healthy individuals, levels of 10 out of the 60 proteins detectable in CSF and plasma (**Table S2**) correlated considerably between the two fluids ($R_s \geq 0.5$; **Fig 5A**). Strikingly, 6 of these 10 correlations were much weaker in AD (FABP3, IL-10, TIMP-1, CCL4 (macrophage inflammatory protein-1 β , MIP-1 β), myoglobin, and TSH. Conversely, levels of intercellular adhesion molecule-1 (ICAM-1) and CCL5 did not correlate between CSF and plasma in NDCs but correlated highly in AD patients (**Fig 5A** and **S1**). Similarly, it becomes apparent that the connectivity network of factors selected in models C1–5 and P6–10 (**Fig 5B,C**) are overall very different in AD and NDC, and this is supported by the change in interaction scores for each factor. Many of the factors appearing as well-connected network hubs in healthy individuals (e.g. insulin, α -fetoprotein, FABP3, or SCF) have very low connectivity in AD patients. In turn, MCSF and CRP have high positive correlations in AD but negative or fewer correlations in NDC. Together, these analyses across the BBB support the notion that the disease process in AD is accompanied by changes in secreted signaling proteins in CSF and plasma.

DISCUSSION

The study of genetic forms of AD has greatly advanced our knowledge about disease processes linked to the disease but the cause of sporadic forms of AD affecting >95% of all patients is unknown. One reason may be that studying this disease is typically limited to imaging or psychometric testing of patients. Also, existing *in vitro* or transgenic animal models based on genetic forms of AD provide limited unbiased information on molecular or cellular networks involved in the pathogenesis of sporadic AD. Here we analyzed AD in a more continuous and complex fashion based on the hypothesis that the systemic network of the extracellular signaling proteome is linked with the pathological traits in AD. To test this hypothesis we modeled known and accepted pathological indicators of the disease (A β 42, t-tau, p-tau₁₈₁, or ratios A β 42/t-tau or A β 42/p-tau₁₈₁) (4, 5) with other CSF or plasma proteins (**Fig 1** and **Table S2**) using the penalized linear regression method E-net (27). We also correlated levels of proteins measured in CSF and plasma with each other and analyzed how the connectivity or “network” of correlations between these factors changes with disease (**Fig 1**). The current study attempts therefore to provide methods for discovery of potentially diagnostic or biologically relevant proteins in AD.

We discovered several small groups of proteins in CSF which could be used to model or predict levels of pathological markers and classify AD and non-demented controls with similar or

better diagnostic utility than the CSF pathological markers themselves (**Fig 2A,B** and **Table II**). These proteins alone or in combination may therefore be associated with the disease process either in a direct or indirect way [see also discussion on fluid biomarkers in relation to AD pathology in (6)], and future experimental studies will need to test this. Consistent with their ability to model CSF tau and A β , several of the selected CSF communicate proteins correlate with these markers and it is striking that most correlations are prominently changed in AD patients (**Fig 2C,D**). This is particularly obvious for correlations between FABP3 or SCF, and pathological markers. FABP3, which shows many strong correlations with other proteins and functions as a network hub, is a cytosolic protein involved in cellular fatty acid uptake, transport, and metabolism (32). It is highly expressed in the adult human brain (33) and has previously been suggested to be a peripheral marker for mild traumatic brain injury and stroke (33-35). In support of a possible change in the half-life of FABP3 in brain and the systemic environment in disease, we observed a moderate positive correlation between CSF and blood FABP3 levels in NDC but a negative correlation in AD patients (**Fig 5A** and **S1**). FABP3 was also independently identified as a possible predictor of AD in a recent ELISA study (36) and two studies of CSF communicate proteins using the same platform that was used in our study (15, 37). Other proteins overlapping between our analysis and the latter two studies include IL-7, SCF, and CCL11/eotaxin (with Hu et al. identifying its close relative Eotaxin-3/CCL26).

Using levels of plasma communicate proteins to model AD pathological markers we identified between 4 and 15 proteins (out of 74 detectable proteins; **Table S2**) for the various models P6-P10. The selected proteins were slightly weaker in their diagnostic utility than the ones selected in CSF models C2, C4, and C5 but outperformed models C1 and C3 (**Table II**). All plasma models required age and *APOE4* status as parameters to achieve sufficient classification accuracy (**Fig 3** and **Table II**). Further validation of the models in an independent test set resulted in reduced AUC values but a clear improvement over the classification accuracy with *APOE4* status and age. Since each of the 5 plasma models was developed independently with the E-net tool, it is reassuring that several proteins were selected in 3, 4 or even all models (shades of orange in **Table 1**). Of these, MCSF and G-CSF may be particularly relevant in AD, as they are reduced in AD plasma (17) and systemic administration of either MCSF (38) or G-CSF (39) ameliorated memory deficits in mouse models of the disease. Furthermore, MCSF functions as a network hub and shows strong positive correlations with FABP3, SCF, and MMP-3 in the CSF-plasma connectivity diagram in AD patients but not in NDC (**Fig 5B,C**).

The comparison of individual correlations of communicate proteins between CSF and plasma in AD and NDC (**Fig 5A**) resulted in an additional set of proteins which overlapped in part

with those identified in models C1–C5 (FABP3, CRP) and P6–P10 (CCL2) as well as proteins reported in the literature as having a role in AD (CCL5, ICAM-1, leptin). Notably, many of these correlations are different in AD compared with NDC. Whether the correlations between CSF and plasma are the result of exchange between the compartments or co-regulation of these proteins and why the correlations change with disease needs to be explored mechanistically. It is reassuring that out of a 18 protein signature we previously described to classify AD or model progression (17) all 6 proteins that were detectable on the two distinct platforms were selected in at least one model here (CCL5, CXCL8, GCSF, ICAM-1, IL-3, MCSF). Likewise, in a recent study that used the multiplex sandwich immunoassay platform to measure 108 serum proteins (including the ones measured here) (16), several predictors of AD overlapped with the ones identified here (e.g. CK-MB, G-CSF).

In the future, the analytical methods described here could be improved by increasing the number of communication factors measured in the plasma or CSF and modeling not only pathological CSF markers but clinical or imaging parameters as well. This could strengthen the value of biological information obtained with this approach. At the same time, this analytical method could go beyond the communicate as we know it today by combining it with the analysis of cellular networks (40) or other "–omic" approaches (41) to discover associations with disease patterns in tissue. Naturally, these methods are not limited to AD but could be used for other diseases where direct access to the diseased organ is difficult. Ultimately, the proteins and biological pathways identified by these analytical approaches need to be validated using appropriate disease models and ultimately, human studies.

In summary, we measured with a targeted proteomic multiplex assay soluble proteins involved in intercellular communication in CSF and plasma of AD patients and cognitively normal elderly controls. We identified with a high-dimensional linear regression method those proteins that are associated with CSF levels of A β and tau, which are pathologically changed in AD, and show AD-related changes in correlations and connectivity networks between these identified proteins within CSF, plasma, or across the BBB. We propose that these network-based analytical approaches can help identify proteins or signaling pathways involved in AD or other chronic neurodegenerative disorders with higher confidence than traditional two-class, disease/control modeling approaches. Future studies need to replicate our findings in large multi-center cohorts and test the various proteins for the biological role in AD.

REFERENCES

1. Steinman, L. (2008) Nuanced roles of cytokines in three major human brain disorders. *J Clin Invest* 118, 3557-3563
2. Perry, V. H., Cunningham, C., and Holmes, C. (2007) Systemic infections and inflammation affect chronic neurodegeneration. *Nat Rev Immunol* 7, 161-167
3. Alzheimer's Association National Office (2011) 2011 Alzheimer's Disease Facts and Figures. Alzheimer's Association National Office, IL
4. Dubois, B., Feldman, H. H., Jacova, C., Cummings, J. L., Dekosky, S. T., Barberger-Gateau, P., Delacourte, A., Frisoni, G., Fox, N. C., Galasko, D., Gauthier, S., Hampel, H., Jicha, G. A., Meguro, K., O'Brien, J., Pasquier, F., Robert, P., Rossor, M., Salloway, S., Sarazin, M., de Souza, L. C., Stern, Y., Visser, P. J., and Scheltens, P. (2010) Revising the definition of Alzheimer's disease: a new lexicon. *Lancet Neurol* 9, 1118-1127
5. Dubois, B., Feldman, H. H., Jacova, C., Dekosky, S. T., Barberger-Gateau, P., Cummings, J., Delacourte, A., Galasko, D., Gauthier, S., Jicha, G., Meguro, K., O'Brien, J., Pasquier, F., Robert, P., Rossor, M., Salloway, S., Stern, Y., Visser, P. J., and Scheltens, P. (2007) Research criteria for the diagnosis of Alzheimer's disease: revising the NINCDS-ADRDA criteria. *Lancet Neurol* 6, 734-746
6. Perrin, R. J., Fagan, A. M., and Holtzman, D. M. (2009) Multimodal techniques for diagnosis and prognosis of Alzheimer's disease. *Nature* 461, 916-922
7. De Meyer, G., Shapiro, F., Vanderstichele, H., Vanmechelen, E., Engelborghs, S., De Deyn, P. P., Coart, E., Hansson, O., Minthon, L., Zetterberg, H., Blennow, K., Shaw, L., and Trojanowski, J. Q. (2010) Diagnosis-independent Alzheimer disease biomarker signature in cognitively normal elderly people. *Arch Neurol* 67, 949-956
8. Shaw, L. M., Vanderstichele, H., Knapik-Czajka, M., Clark, C. M., Aisen, P. S., Petersen, R. C., Blennow, K., Soares, H., Simon, A., Lewczuk, P., Dean, R., Siemers, E., Potter, W., Lee, V. M., and Trojanowski, J. Q. (2009) Cerebrospinal fluid biomarker signature in Alzheimer's disease neuroimaging initiative subjects. *Ann Neurol* 65, 403-413
9. Visser, P. J., Verhey, F., Knol, D. L., Scheltens, P., Wahlund, L. O., Freund-Levi, Y., Tsolaki, M., Minthon, L., Wallin, A. K., Hampel, H., Burger, K., Pirttila, T., Soininen, H., Rikkert, M. O., Verbeek, M. M., Spira, L., and Blennow, K. (2009) Prevalence and prognostic value of CSF markers of Alzheimer's disease pathology in patients with subjective cognitive impairment or mild cognitive impairment in the DESCRIPA study: a prospective cohort study. *Lancet Neurol* 8, 619-627
10. Fagan, A. M., Roe, C. M., Xiong, C., Mintun, M. A., Morris, J. C., and Holtzman, D. M. (2007) Cerebrospinal fluid tau/beta-amyloid(42) ratio as a prediction of cognitive decline in nondemented older adults. *Arch Neurol* 64, 343-349
11. Li, G., Sokal, I., Quinn, J. F., Leverenz, J. B., Brodey, M., Schellenberg, G. D., Kaye, J. A., Raskind, M. A., Zhang, J., Peskind, E. R., and Montine, T. J. (2007) CSF tau/Abeta42 ratio for increased risk of mild cognitive impairment: a follow-up study. *Neurology* 69, 631-639
12. Okonkwo, O. C., Alosco, M. L., Griffith, H. R., Mielke, M. M., Shaw, L. M., Trojanowski, J. Q., and Tremont, G. (2010) Cerebrospinal fluid abnormalities and rate of decline in everyday function across the dementia spectrum: normal aging, mild cognitive impairment, and Alzheimer disease.

13. Fagan, A. M., Head, D., Shah, A. R., Marcus, D., Mintun, M., Morris, J. C., and Holtzman, D. M. (2009) Decreased cerebrospinal fluid Abeta(42) correlates with brain atrophy in cognitively normal elderly. *Ann Neurol* 65, 176-183
14. Britschgi, M., and Wyss-Coray, T. (2007) Systemic and acquired immune responses in Alzheimer's disease. *Int Rev Neurobiol* 82, 205-233
15. Hu, W. T., Chen-Plotkin, A., Arnold, S. E., Grossman, M., Clark, C. M., Shaw, L. M., Pickering, E., Kuhn, M., Chen, Y., McCluskey, L., Elman, L., Karlawish, J., Hurtig, H. I., Siderowf, A., Lee, V. M., Soares, H., and Trojanowski, J. Q. (2010) Novel CSF biomarkers for Alzheimer's disease and mild cognitive impairment. *Acta Neuropathol* 119, 669-678
16. O'Bryant, S. E., Xiao, G., Barber, R., Reisch, J., Doody, R., Fairchild, T., Adams, P., Waring, S., and Diaz-Arrastia, R. (2010) A serum protein-based algorithm for the detection of Alzheimer disease. *Arch Neurol* 67, 1077-1081
17. Ray, S., Britschgi, M., Herbert, C., Takeda-Uchimura, Y., Boxer, A., Blennow, K., Friedman, L. F., Galasko, D. R., Jutel, M., Karydas, A., Kaye, J. A., Leszek, J., Miller, B. L., Minthon, L., Quinn, J. F., Rabinovici, G. D., Robinson, W. H., Sabbagh, M. N., So, Y. T., Sparks, D. L., Tabaton, M., Tinklenberg, J., Yesavage, J. A., Tibshirani, R., and Wyss-Coray, T. (2007) Classification and prediction of clinical Alzheimer's diagnosis based on plasma signaling proteins. *Nat Med* 13, 1359-1362
18. Soares, H. D., Chen, Y., Sabbagh, M., Roher, A., Schrijvers, E., and Breteler, M. (2009) Identifying early markers of Alzheimer's disease using quantitative multiplex proteomic immunoassay panels. *Ann N Y Acad Sci* 1180, 56-67
19. Zhang, J., Sokal, I., Peskind, E. R., Quinn, J. F., Jankovic, J., Kenney, C., Chung, K. A., Millard, S. P., Nutt, J. G., and Montine, T. J. (2008) CSF multianalyte profile distinguishes Alzheimer and Parkinson diseases. *Am J Clin Pathol* 129, 526-529
20. Booij, B. B., Lindahl, T., Wetterberg, P., Skaane, N. V., Saebo, S., Feten, G., Rye, P. D., Kristiansen, L. I., Hagen, N., Jensen, M., Bardsen, K., Winblad, B., Sharma, P., and Lonneborg, A. (2011) A gene expression pattern in blood for the early detection of Alzheimer's disease. *J Alzheimers Dis* 23, 109-119
21. Rye, P. D., Booij, B. B., Grave, G., Lindahl, T., Kristiansen, L., Andersen, H. M., Horndalsveen, P. O., Nygaard, H. A., Naik, M., Hoprekstad, D., Wetterberg, P., Nilsson, C., Aarsland, D., Sharma, P., and Lonneborg, A. (2011) A novel blood test for the early detection of Alzheimer's disease. *J Alzheimers Dis* 23, 121-129
22. Lucin, K. M., and Wyss-Coray, T. (2009) Immune activation in brain aging and neurodegeneration: too much or too little? *Neuron* 64, 110-122
23. Hixson, J. E., and Vernier, D. T. (1990) Restriction isotyping of human apolipoprotein E by gene amplification and cleavage with HhaI. *J Lipid Res* 31, 545-548
24. Li, G., Peskind, E. R., Millard, S. P., Chi, P., Sokal, I., Yu, C. E., Bekris, L. M., Raskind, M. A., Galasko, D. R., and Montine, T. J. (2009) Cerebrospinal fluid concentration of brain-derived neurotrophic factor and cognitive function in non-demented subjects. *PLoS One* 4, e5424
25. R Development Core Team (2009) R: A language and environment for statistical computing., R Foundation for Statistical Computing, Vienna, Austria
26. van den Berg, R. A., Hoefsloot, H. C., Westerhuis, J. A., Smilde, A. K., and van der Werf, M. J. (2006) Centering, scaling, and transformations: improving the biological information content of metabolomics data. *BMC Genomics* 7, 142

27. Zou, H., and Hastie, T. (2005) Regularization and variable selection via the elastic net. *Journal of the Royal Statistical Society: Series B (Statistical Methodology)* 67, 301-320
28. Friedman, J., Hastie, T., and Tibshirani, R. (2010) Regularization paths for generalized linear models via coordinate descent. *J Stat Software* 33, 1-22
29. Hanley, J. A., and McNeil, B. J. (1982) The meaning and use of the area under a receiver operating characteristic (ROC) curve. *Radiology* 143, 29-36
30. Pepe, M. (2003) *The statistical evaluation of medical tests for classification and prediction*, Oxford University Press
31. Blennow, K., and Hampel, H. (2003) CSF markers for incipient Alzheimer's disease. *Lancet Neurol* 2, 605-613
32. Veerkamp, J. H., and Zimmerman, A. W. (2001) Fatty acid-binding proteins of nervous tissue. *J Mol Neurosci* 16, 133-142
33. Pelsers, M. M., Hanhoff, T., Van der Voort, D., Arts, B., Peters, M., Ponds, R., Honig, A., Rudzinski, W., Spener, F., de Kruijk, J. R., Twijnstra, A., Hermens, W. T., Menheere, P. P., and Glatz, J. F. (2004) Brain- and heart-type fatty acid-binding proteins in the brain: tissue distribution and clinical utility. *Clin Chem* 50, 1568-1575
34. Wunderlich, M. T., Hanhoff, T., Goertler, M., Spener, F., Glatz, J. F., Wallesch, C. W., and Pelsers, M. M. (2005) Release of brain-type and heart-type fatty acid-binding proteins in serum after acute ischaemic stroke. *J Neurol* 252, 718-724
35. Zimmermann-Ivol, C. G., Burkhard, P. R., Le Floch-Rohr, J., Allard, L., Hochstrasser, D. F., and Sanchez, J. C. (2004) Fatty acid binding protein as a serum marker for the early diagnosis of stroke: a pilot study. *Mol Cell Proteomics* 3, 66-72
36. Chiasserini, D., Parnetti, L., Andreasson, U., Zetterberg, H., Giannandrea, D., Calabresi, P., and Blennow, K. (2010) CSF levels of heart fatty acid binding protein are altered during early phases of Alzheimer's disease. *J Alzheimers Dis* 22, 1281-1288
37. Hu, W. T., Chen-Plotkin, A., Arnold, S. E., Grossman, M., Clark, C. M., Shaw, L. M., McCluskey, L., Elman, L., Karlawish, J., Hurtig, H. I., Siderowf, A., Lee, V. M., Soares, H., and Trojanowski, J. Q. (2010) Biomarker discovery for Alzheimer's disease, frontotemporal lobar degeneration, and Parkinson's disease. *Acta Neuropathol* 120, 385-399
38. Boissonneault, V., Filali, M., Lessard, M., Relton, J., Wong, G., and Rivest, S. (2009) Powerful beneficial effects of macrophage colony-stimulating factor on beta-amyloid deposition and cognitive impairment in Alzheimer's disease. *Brain* 132, 1078-1092
39. Tsai, K. J., Tsai, Y. C., and Shen, C. K. (2007) G-CSF rescues the memory impairment of animal models of Alzheimer's disease. *J Exp Med* 204, 1273-1280
40. Park, J., Lee, D. S., Christakis, N. A., and Barabasi, A. L. (2009) The impact of cellular networks on disease comorbidity. *Mol Syst Biol* 5, 262
41. Inouye, M., Kettunen, J., Soininen, P., Silander, K., Ripatti, S., Kumpula, L. S., Hamalainen, E., Jousilahti, P., Kangas, A. J., Mannisto, S., Savolainen, M. J., Jula, A., Leiviska, J., Palotie, A., Salomaa, V., Perola, M., Ala-Korpela, M., and Peltonen, L. (2010) Metabonomic, transcriptomic, and genomic variation of a population cohort. *Mol Syst Biol* 6, 441

ACKNOWLEDGMENTS

We are grateful to the individuals who participated in this study. We also thank H. Johns for technical assistance and S.D. Edland for support in accessing the database and acknowledge numerous unnamed staff at our institutions for their effort in patient recruitment, clinical assessment and sample preparation. This study was supported by the Stanford University School of Medicine Med Scholars Program Grant (SLBH), Anonymous (TWC), the Department of Veterans Affairs (TWC, ERP, GL), and the US National Institute on Aging (AG27505, TWC; AG10491, AG05136, ERP; AG08017, JFQ and JAK; AG05131 and AGO23185, DRG).

AUTHORS' CONTRIBUTION

MB and TWC designed the study and wrote the paper. MB, KR, and TWC prepared the statistical analysis plan, KR did the statistical analysis, and MB and TWC did the network analysis and the further interpretation of the data. SLBH contributed to data analysis. CMC, DRG, JAK, GL, ERP, and JFQ provided plasma and CSF samples, did measurements of A β 42, total tau, and p-tau₁₈₁, identified patients and controls, and were responsible for collecting data from them.

CONFLICT OF INTEREST

The authors do not report a conflict of interest.

FIGURE LEGENDS

Fig 1. Modeling of pathological markers in CSF and classification of AD based on communication factors in CSF and plasma. Accumulation of plaques and tangles in the AD brain is associated with decreased levels of A β and increased levels of tau in CSF, respectively (green dashed double arrow). Relative levels of these proteins alone or their ratios can be used to classify AD and NDC (green solid arrow). In Elastic net (E-net) regression models C1–C5 soluble communication factors in CSF (CSF communicome; see text for details) are used to model tau and A β levels or their ratios (dashed purple double arrow) and subsequently to classify AD and NDC (solid purple line). In E-net models P6–P10 soluble communication factors in plasma (plasma communicome) derived from the training set are used to model tau and A β levels or their ratios (dashed red double arrow) and subsequently to classify AD and NDC (solid red line). These variables were validated by classifying AD and NDC in an independent test set. In a separate analysis correlations are studied between CSF communicome proteins and corresponding plasma communicome proteins in AD patients and NDCs (dashed blue double arrow).

Fig 2. Pathology associated CSF communicome models can classify AD and NDC and the connectivity network of the proteins in these models is altered in AD patients. (A, B) CSF pathological markers or CSF Elastic net (E-net) models C2 and C5 were used to calculate ROC curves. The color-coding is based on **Fig 1** and the numbers indicate the AUC values and 95% C.I. (listed also in **Table III**). (A) CSF samples from AD patients and NDC were classified based on levels of CSF p-tau₁₈₁ (solid green line) or levels of CSF communicome proteins (FABP3, CCL11, endothelin-1, CK-MB, IL-13, CXCL8) and *APOE4* status selected in model C2 (dashed purple line). (B) CSF samples from AD patients and NDC were classified based on levels of CSF A β ₄₂/p-tau₁₈₁ (solid green line) or levels of CSF communicome proteins (FABP3, IL-13, SCF, CK-MB, α -fetoprotein, endothelin-1, CRP) and *APOE4* status selected in model C5 (dashed purple line). (C, D) Network diagrams illustrating connectivity between CSF pathological markers and CSF communication factors selected in models C1–C5. The connectivity between two proteins is expressed as Spearman rank correlation coefficient R_s calculated from all measurements for these two proteins in CSF samples of non-demented controls (C) or AD patients (D), respectively. The correlations are visualized in a network with different strokes and colors depending on strength and type of connectivity between proteins. Red strokes $R_s \geq 0.4$, blue strokes $R_s \leq -0.4$. In parentheses next to the name of the analyte is the interaction score, which is the sum of the

squared values of all R_s between all analytes in the connectivity diagram. Note the considerable change of the interaction scores between communication factors in AD patients (**D**) compared with NDC (**C**).

Fig 3. Pathology associated plasma communicome models that efficiently classify AD and NDC are validated in an independent test set. ROC curves for the plasma training and a test set were calculated with CSF pathological markers (solid green lines), AD risk factors *APOE4* status and age (solid black lines), or plasma Elastic net (E-net) models P2 and P5 (dashed red lines), respectively. The color-coding is based on **Fig 1** and the numbers indicate the AUC values and 95% C.I. (listed also in **Table III**). **(A)** AD patients and NDC in the training set were classified based on levels of CSF p-tau₁₈₁ or the variables selected to be associated with p-tau₁₈₁ in e-net model P2: plasma communicome proteins (MCSF, CD40L, G-CSF, adiponectin, CCL2, CK-MB, TNF- β , β 2-microglobulin, TNF RII, IL-4, IL-3, IL-18, PAI-1, Apo CIII, TBG), *APOE4* status, and age. **(B)** The variables selected in the training set E-net model P2 are validated in an independent test set of AD and NDC and compared to the ROC curves that were calculated based either on levels of CSF p-tau₁₈₁ or *APOE4* status and age of 53 of the 65 subjects in the test set; measurements of A β 42 and tau were not done for 6 NDC and 6 AD in the test set. **(C)** AD patients and NDC in the training set were classified based on levels of CSF A β 42/p-tau₁₈₁ or the variables selected to be associated with p-tau₁₈₁ in E-net model P10: plasma communicome proteins (MCSF, G-CSF, GH, TPO), *APOE4* status, and age. **(D)** The variables selected in the training set E-net model P10 are validated in an independent test set of AD and NDC and compared to the ROC curves that were calculated based either on levels of CSF A β 42/p-tau₁₈₁ or *APOE4* status and age of the subjects in the test set. See connectivity network in **Fig 4** for illustration of the changes in interactions between communication factors in AD patients compared with controls.

Fig 4. Plasma predictors of pathological markers point to changes in the communicome network in plasma of AD patients. **(A, B)** Connectivity diagrams of pathological markers in CSF and communication factors in plasma, which were chosen in Elastic net regression models for these markers. The relationship between two proteins is expressed as Spearman rank correlation coefficient R_s calculated from all measurements for these two proteins in non-demented controls **(A)** or AD patients **(B)**, respectively. The correlations are visualized in a network with different strokes and colors depending on strength and type of a relationship between proteins. Red strokes

$R_S \geq 0.4$, blue strokes $R_S \leq -0.4$. In parentheses next to the name of the analyte is the interaction score, which is the sum of the squared values of all R_S between all analytes in the connectivity diagram. Note the considerable difference in connectivity between communication factors in AD patients compared with NDC.

Fig 5. Correlations and connectivity between communication factors in CSF and plasma are different in AD patients compared with NDC. (A) Spearman rank correlations (correlation coefficient R_S) between CSF and plasma in non-demented controls (green bars) and AD patients (blue bars). Proteins with $R_S \geq 0.5$ in at least one group are shown. $R_S \leq -0.5$ were not observed. Note that levels of CCL5 and ICAM-1 correlate much stronger in AD than in NDC across the BBB and that ApoH and CCL2 reach $R_S = 0.5$ in AD but not in NDC. **(B, C)** Connectivity diagrams illustrating correlations between CSF communication factors selected in models C1–C5 and plasma communication factors selected in models P6–P10. In parentheses are the interaction scores. See legend to **Fig 2** for more details on calculations. Note the considerable lack and difference in connectivity between communication factors in AD patients **(C)** compared with NDC **(B)**. See also **Fig S1**. BBB, blood-brain barrier.

Table I. List of variables selected in the Elastic net models.

Variables selected in the models for CSF ^a

Model C1: t-tau	Model C2: p-tau ₁₈₁	Model C3: Aβ42	Model C4: Aβ42/t-tau	Model C5: Aβ42/ p-tau ₁₈₁
FABP3 (0.34)	FABP3 (0.41)	IL-7 (0)	FABP3 (-0.17)	APOE (-0.28)
CK-MB (-0.10)	CCL11 (-0.21)		APOE (-0.15)	FABP3 (-0.10)
	APOE (0.21)		SCF (-0.11)	IL-13 (-0.08)
	Endothelin-1 (0.20)		Endothelin-1 (-0.07)	SCF (-0.08)
	CK-MB (-0.20)		TNF-β (-0.03)	CK-MB (-0.05)
	IL-13 (0.19)		CK-MB (0.03)	α-Fetoprotein (-0.03)
	MMP-3 (0.18)			Endothelin-1 (-0.03)
	CXCL8 (-0.17)			CRP (0.01)
	+18 more ^c			

Variables selected in the models for plasma ^b

Model P6: t-tau	Model P7: p-tau ₁₈₁	Model P8: Aβ42	Model P9: Aβ42/t-tau	Model P10: Aβ42/ p-tau ₁₈₁
TNF RII (0.08)	MCSF (-0.07)	APOE (-0.31)	APOE (-0.32)	APOE (-0.21)
Age (0.06)	CD40L (-0.04)	Age (-0.24)	Age (-0.28)	MCSF (0.15)
MCSF (-0.06)	APOE (0.04)	MCSF (0.15)	MCSF (0.17)	Age (-0.12)
TF (0.06)	G-CSF (-0.04)	IL-18 (0.02)	IL-12 p70 (0.07)	G-CSF (0.12)
IL-3 (0.04)	Adiponectin (0.04)	IL-12 p70 (0.02)	CK-MB (0.04)	GH (0.03)
APOE (0.04)	CCL2 (-0.02)	IgA (0.01)	IL-4 (-0.03)	TPO (0.01)
ApoCIII (-0.02)	CK-MB (-0.02)	CK-MB (<0.01)	TIMP-1 (0.02)	
Adiponectin (0.02)	TNF-β (0.01)		G-CSF (0.02)	
EN-RAGE (0.02)	Age (0.01)		β2-Microglobulin (-0.02)	
G-CSF (-0.02)	β2-Microglobulin (0.01)		TNF RII (-0.01)	
CK-MB (-0.01)	TNF RII (0.01)		EN-RAGE (-0.01)	
Insulin (-0.01)	IL-4 (0.01)		TF (-0.01)	
CD40L (-0.01)	IL-3 (0.01)		PAI-1 (0.01)	
PAI-1 (-0.01)	IL-18		IL-3	
	PAI-1			
	Apo CIII			
	TBG			

^a Based on the CSF set with 43 subjects, AD n = 25, NDC n = 18 subjects.

^b Based on the training set with 131 subjects, AD n = 52, NDC n = 79 subjects.

^c In model C2 the E-net chose 26 predictors for modeling p-tau_{181p} with CSF proteins and subjects' characteristics. To avoid overfitting for this model we limited the number of selected variables to 8. The additional 18 variables in order of how they were selected by the E-net here in an extended list: CRP, age, VEGF, SCF, CA19-9, IL-10, IL-5, C3, haptoglobin, TBG, calcitonin, GST, CCL2, α-fetoprotein, PAPP-A, ApoA1, CCL3, IgM.

^d Note that for Aβ42 only one variable was selected with a very small estimated regression coefficient.

All values were standardized and penalized linear regression models were calculated with the E-net method. Response variables: t-tau, p-tau₁₈₁, Aβ42, or the ratios of Aβ42/t-tau, or Aβ42/p-tau₁₈₁. Explanatory variables: CSF or plasma protein levels together with sex and risk factors for AD APOE genotype and age. For each response a separate model was calculated (Model C1-5 in CSF, P6-8 in plasma) and variables that fitted best into the corresponding model are listed in order of decreasing absolute size of the estimated regression coefficient (RC, indicated in parentheses). Since all variables had been standardized, the RC serves as a measure of the strength for the association between an explanatory variable and its corresponding response variable: the larger RC in absolute value, the higher the association to the response. A RC close to 0 points to a low degree of association between the corresponding variable and the response. For protein nomenclature see **Table S2**.

Suggested location in the text: Results, after second subtitle

Table II. Classification of AD and non-demented controls.

CSF sample set (n = 43)			
Established biomarker model	AUC calculated based on established biomarkers in CSF ^a	E-net model	AUC calculated based on CSF communicome, age, and <i>APOE4</i> status ^b
t-tau	0.86 (0.71-0.94)	C1	0.75 (0.56-0.88)
p-tau ₁₈₁	0.90 (0.74-0.97)	C2	0.88 (0.70-0.96)
Aβ1-42	0.75 (0.58-0.87)	C3	n.a.
Aβ1-42/t-tau	0.84 (0.69-0.93)	C4	0.91 (0.77-0.97)
Aβ1-42/p-tau ₁₈₁	0.86 (0.70-0.94)	C5	0.93 (0.78-0.98)

Training set (n = 131)			
Established biomarker model	AUC calculated based on established biomarkers in CSF ^a	E-net model	AUC calculated based on plasma communicome, age, and <i>APOE4</i> status ^b
t-tau	0.80 (0.71-0.87)	P6	0.86 (0.79-0.92)
p-tau ₁₈₁	0.82 (0.73-0.89)	P7	0.86 (0.78-0.92)
Aβ1-42	0.81 (0.72-0.87)	P8	0.85 (0.76-0.90)
Aβ1-42/t-tau	0.85 (0.78-0.91)	P9	0.86 (0.78-0.92)
Aβ1-42/p-tau ₁₈₁	0.84 (0.76-0.90)	P10	0.84 (0.76-0.90)

Test set (n = 65)			
Established biomarker model	AUC calculated based on established biomarkers in CSF ^c	Validation of variables selected in E-net model	AUC calculated based on plasma communicome, age, and <i>APOE4</i> status selected in the training set ^d
t-tau	0.80 (0.630-0.907)	P6	0.77 (0.63-0.87)
p-tau ₁₈₁	0.81 (0.648-0.909)	P7	0.76 (0.61-0.86)
Aβ1-42	0.84 (0.704-0.925)	P8	0.75 (0.60-0.85)
Aβ1-42/t-tau	0.86 (0.715-0.938)	P9	0.77 (0.63-0.87)
Aβ1-42/p-tau ₁₈₁	0.86 (0.725-0.934)	P10	0.74 (0.60-0.85)

^a AUC calculated based on the levels of established pathological CSF biomarkers t-tau, p-tau₁₈₁, Aβ1-42 and their ratios in subjects used for CSF or plasma models, respectively.

^b AUC (in bold) calculated based on communicome, age and *APOE4* status and their corresponding regression coefficients as selected in Elastic net (E-net) models C1-5 (CSF) and P6-10 (plasma) in subjects used for CSF or plasma models, respectively. Note that for Aβ1-42 only IL-7 with a regression coefficient close to 0 was selected in the E-net model C3. Thus, no ROC/AUC could be calculated (n.a., not applicable).

^c These AUC results are based on 53 subjects because 6 controls and 6 AD patients had no measurement of Aβ and tau in CSF.

^d Variables selected by the E-net models P6-10 in the training set were validated in an independent test set and AUC was calculated for all 65 subjects (italicized and bold).

Compare AUC calculated using variables selected in elastic net models (**Table I**) with AUC calculated using established markers for pathology. See also ROC curves in **Figures 2 and 3**.

Suggested location in the text: Results, after Table I

Fig 1. Modeling of pathological markers in CSF and classification of AD based on communication factors in CSF and plasma.

Suggested location in the text: Results, before second subtitle

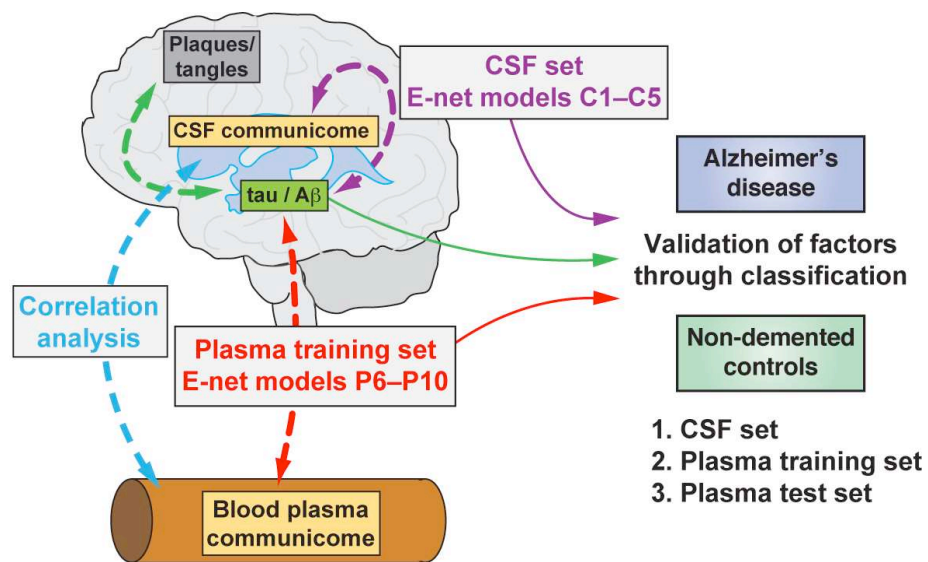


Figure 1, Britschgi et al.

Fig 2. Pathology associated CSF communicate models can classify AD and NDC and the connectivity network of the proteins in these models is altered in AD patients.

Suggested location in the text: Results, before third subtitle

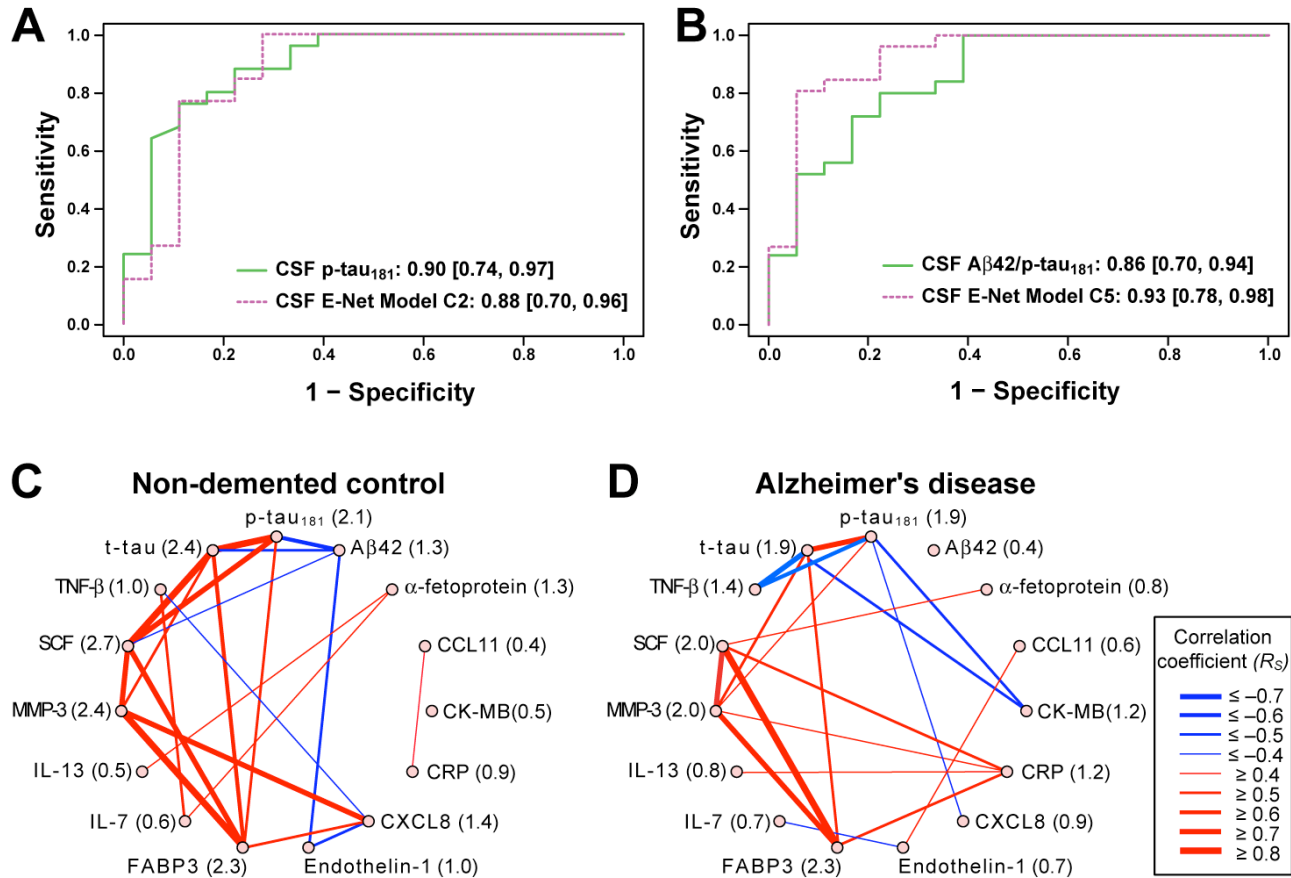


Figure 2, Britschgi et al.

Fig 3. Pathology associated plasma communicate models that efficiently classify AD and NDC are validated in an independent test set.

Suggested location in the text: Results, before fourth subtitle

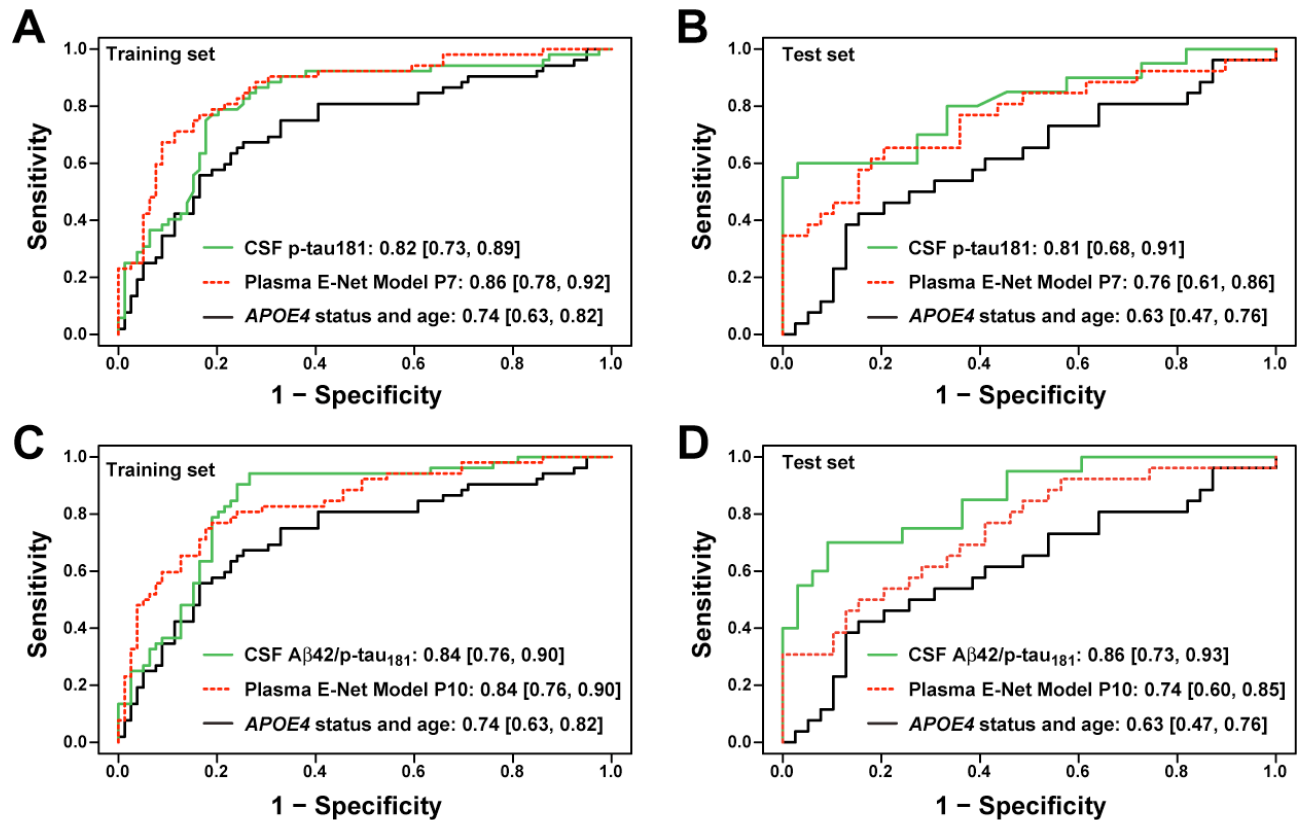


Figure 3, Britschgi et al.

Fig 4. Plasma predictors of pathological markers point to changes in the communicome network in plasma of AD patients.

Suggested location in the text: Results, right after Figure 3

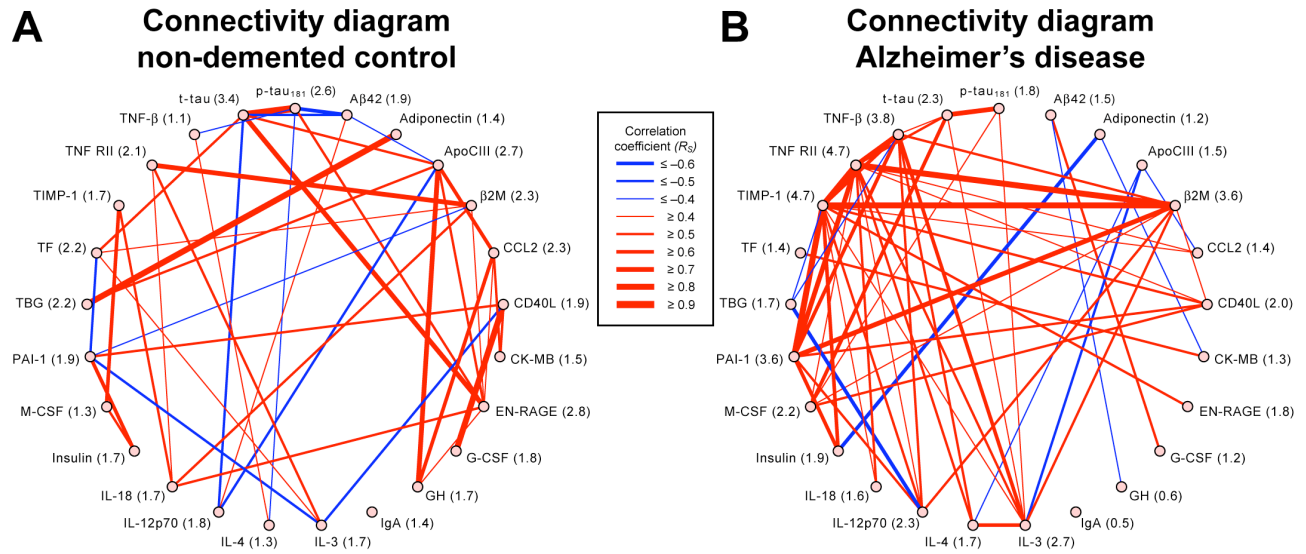


Fig 5. Correlations and connectivity between communication factors in CSF and plasma are different in AD patients compared with NDC.

Suggested location in the text: Results, before discussion

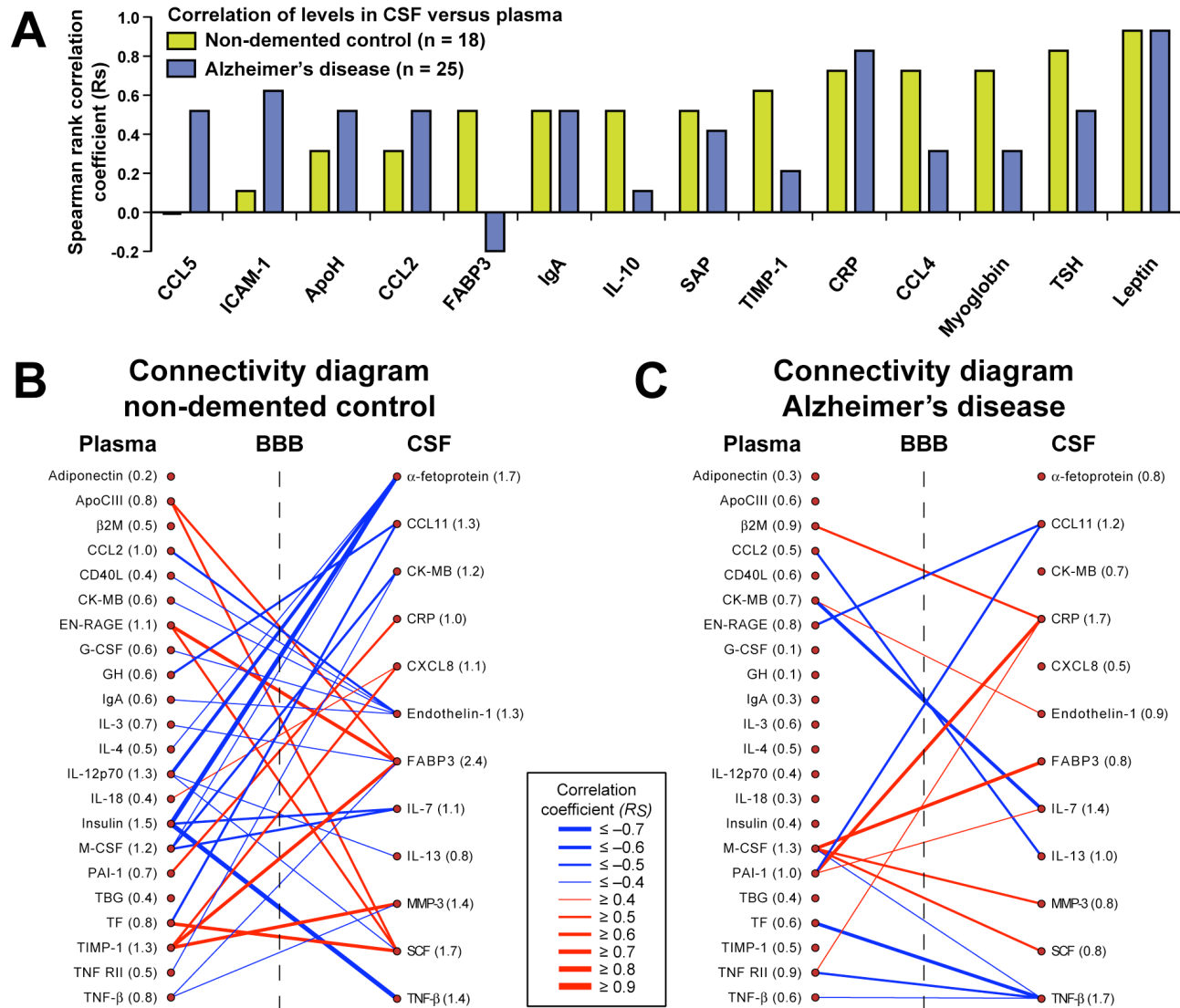


Figure 5, Britschgi et al.